

## Comparative analysis of Venus and Mars magnetotails

A. Fedorov<sup>a,\*</sup>, C. Ferrier<sup>a</sup>, J.A. Sauvaud<sup>a</sup>, S. Barabash<sup>b</sup>, T.L. Zhang<sup>c</sup>, C. Mazelle<sup>a</sup>, R. Lundin<sup>b</sup>, H. Gunell<sup>b</sup>, H. Andersson<sup>b</sup>, K. Brinkfeldt<sup>b</sup>, Y. Futaana<sup>b</sup>, A. Grigoriev<sup>b</sup>, M. Holmström<sup>b</sup>, M. Yamauchi<sup>b</sup>, K. Asamura<sup>d</sup>, W. Baumjohann<sup>c</sup>, H. Lammer<sup>c</sup>, A.J. Coates<sup>e</sup>, D.O. Kataria<sup>e</sup>, D.R. Linder<sup>e</sup>, C.C. Curtis<sup>f</sup>, K.C. Hsieh<sup>f</sup>, B.R. Sandel<sup>f</sup>, J.-J. Thocaven<sup>a</sup>, M. Grande<sup>g</sup>, H. Koskinen<sup>h</sup>, E. Kallio<sup>i</sup>, T. Sales<sup>i</sup>, W. Schmidt<sup>i</sup>, P. Riihela<sup>i</sup>, J. Kozyra<sup>j</sup>, N. Krupp<sup>k</sup>, J. Woch<sup>k</sup>, J. Luhmann<sup>l</sup>, S. McKenna-Lawlor<sup>m</sup>, S. Orsini<sup>n</sup>, R. Cerulli-Irelli<sup>n</sup>, A. Mura<sup>n</sup>, A. Milillo<sup>n</sup>, M. Maggi<sup>n</sup>, E. Roelof<sup>o</sup>, P. Brandt<sup>o</sup>, C.T. Russell<sup>p</sup>, K. Szego<sup>q</sup>, J.D. Winningham<sup>r</sup>, R.A. Frahm<sup>r</sup>, J. Scherrer<sup>r</sup>, J.R. Sharber<sup>r</sup>, P. Wurz<sup>s</sup>, P. Bochsler<sup>s</sup>

<sup>a</sup>Centre d'Etude Spatiale des Rayonnements 31028, Toulouse, France

<sup>b</sup>Swedish Institute of Space Physics, S-98 128 Kiruna, Sweden

<sup>c</sup>Space Research Institute, Austrian Academy of Sciences, OAW, Graz, Austria

<sup>d</sup>Institute of Space and Astronautical Science, 3-1-1 Yoshinodai, Sagamihara, Japan

<sup>e</sup>Mullard Space Science Laboratory, University College London, Surrey RH5 6NT, UK

<sup>f</sup>University of Arizona, Tucson, AZ 85721, USA

<sup>g</sup>Rutherford Appleton Laboratory, Chilton, Didcot, Oxfordshire OX11 0QX, UK

<sup>h</sup>Department of Physical Sciences, University of Helsinki, P.O. Box 64, 00014 Helsinki, Finland

<sup>i</sup>Finnish Meteorological Institute, Box 503, FIN-00101 Helsinki, Finland

<sup>j</sup>Space Physics Research Laboratory, University of Michigan, Ann Arbor, MI 48109-2143, USA

<sup>k</sup>Max-Planck-Institut fuer Sonnensystemforschung, D-37191 Katlenburg-Lindau, Germany

<sup>l</sup>Space Science Laboratory, University of California at Berkeley, Berkeley, CA 94720-7450, USA

<sup>m</sup>Space Technology Ireland, National University of Ireland, Maynooth, Co. Kildare, Ireland

<sup>n</sup>Instituto di Fisica dello Spazio Interplanetari, I-00133 Rome, Italy

<sup>o</sup>Applied Physics Laboratory, Johns Hopkins University, Laurel, MD 20723-6099, USA

<sup>p</sup>Institute of Geophysics and Planetary Physics, University of California, 405 Hilgard Ave Los Angeles, CA 90095-1567, USA

<sup>q</sup>KFKI Research Institute for Particle and Nuclear Physics, Box 49, H-1525 Budapest, Hungary

<sup>r</sup>Southwest Research Institute, San Antonio, TX 7228-0510, USA

<sup>s</sup>University of Bern, Physikalisches Institut, CH-3012 Bern, Switzerland

Accepted 26 September 2007

Available online 2 January 2008

### Abstract

We have an unique opportunity to compare the magnetospheres of two non-magnetic planets as Mars and Venus with identical instrument sets Aspera-3 and Aspera-4 on board of the Mars Express and Venus Express missions. We have performed both statistical and case studies of properties of the magnetosheath ion flows and the flows of planetary ions behind both planets. We have shown that the general morphology of both magnetotails is generally identical. In both cases the energy of the light ( $H^+$ ) and the heavy ( $O^+$ , etc.) ions decreases from the tail periphery (several keV) down to few eV in the tail center. At the same time the wake center of both planets is occupied by plasma sheet coincident with the current sheet of the tail. Both plasma sheets are filled by accelerated (500–1000 eV) heavy planetary ions. We report also the discovery of a new feature never observed before in the tails of non-magnetic planets: the plasma sheet is enveloped by consecutive layers of  $He^+$  and  $H^+$  with decreasing energies.

© 2007 Elsevier Ltd. All rights reserved.

**Keywords:** Mars; Venus; Magnetotail; Magnetosphere

\*Corresponding author.

E-mail address: [Andrei.Fedorov@cesr.fr](mailto:Andrei.Fedorov@cesr.fr) (A. Fedorov).

## 1. Introduction

There are two essential effects inherent to the interaction of non-magnetic bodies with solar wind: (1) generation of the planetary magnetosphere by the currents induced in the superconducting ionosphere and (2) mass loading of the incident solar wind by a continuously ionizing exosphere. Both effects alter the solar wind magnetic field and create the solar wind void near the planet body. Mass loading and the direct interaction of the interplanetary magnetic field (IMF) with the ionospheres fill these voids by accelerated planetary ions. The first model of formation of such a void and generation of its rather sharp boundary was proposed by Vaisberg and Zeleny (1984) and Vaisberg et al. (1989). Mass loading is the main type of interaction of the solar wind with comets (Alfvén, 1957). At solar maximum Venus is an example of another extreme case (Luhmann et al., 2004) when the whole solar wind dynamic pressure is balanced by the thermal pressure of ionosphere. Mars has an extended hydrogen exosphere which mass loads and decelerates the incident solar wind far away from the ionosphere. As a result the Martian induced magnetosphere can be greater than Venusian magnetosphere as scaled by the planetary radius.

Martian magnetosphere has been studied with the Phobos mission (ASPERA instrument, see Lundin et al., 1998), and then with the Mars Express (MEX) mission (ASPERA-3, see Barabash et al., 2004). The magnetic morphology of the Venus wake has been studied in details by the Pioneer Venus Orbiter (PVO) (see McComas et al., 1986). The presence of heavy ions in the Venusian magnetotail (Moore et al., 1990) was inferred from Orbiter Plasma Analyzer data onboard of PVO, but this instrument was not a real ion composition analyzer. The Venus Express (VEX) mission includes a mass spectrometer, an electron spectrometer, and a magnetometer, allowing for a comprehensive investigation of the Venus magnetotail.

The present paper is a first attempt to compare nightside magnetospheres of Venus and Mars on the base of the MEX and VEX observations. To do this we used both statistical and case studies.

## 2. Data sets and data analysis technique

This work is based on the data of the mass spectrometer IMA, identical in both plasma packages ASPERA-3 on board of MEX and ASPERA-4 on VEX. We also use the data of the MAG magnetometer aboard of VEX. IMA has almost a  $4\pi$  field of view with angular resolution equal to  $22\frac{1}{2} \times 6\frac{1}{2}$ . The energy range of the sensor is 12–30 000 eV/charge (35 eV/charge is the low limit in the case of MEX). The instrument can resolve solar wind ions:  $H^+$  and  $He^{++}$ , and planetary origin ions:  $O^+$ ,  $O_2^+$ , and  $He^+$ . Accumulation of one complete angular-energy-mass spectrum takes 192 s. For further details see Barabash et al. (2004). The magnetometer (see Zhang et al., 2006) provides at least 1 Hz magnetic field vector with accuracy better than 1 nT.

For the statistical part of this study we use more than 2 years (2004–2006) of MEX observations and 50 VEX orbits (from August 1st to September 18, 2006). We use only data collected on the nightside partition of the orbits.

Present paper deals with the fluxes and energies of specific ion species in the solar wind and in the planetary magnetospheres. To extract the flux of the selected ion we processed each of 192 s spectrum as follows: (1) we selected the ion distribution core (or several cores) of the 4-D energy-angular-mass original spectrum and intergrated the result over the angular range; (2) for each energy step of the resulting energy-mass spectrum we separated the main expected ions, namely:  $H^+$ ,  $He^{++}$ ,  $He^+$ ,  $O^+$ ,  $O_2^+$  by the best fit of corresponding Gaussian peaks. This procedure results in five energy differential spectra  $D_m(E/Q)$  (intergrated over the sphere). Here  $m$  is an ion specie index. Further statistical study has been performed with total fluxes  $F_m = \int D_m(E/Q) dE/Q$  and mean energies  $E0_m = MV0_m^2/2$ , where  $V0 = \int (D(V)/V^2 V dV) / \int (D(V)/V^2 dV)$ .

We used a superposed epoch technique to get spatial distributions of ion flows shown in the next sections. Flux values have been accumulated and averaged in a  $0.06 \times 0.06R$  grid, where  $R$  is a planet radius. Each 192 s spectrum corresponds to finite part of the orbit. To fill the proper cells we uniformly distributed the measured flux value over a curve strip of  $0.06R$  width located along the orbit segment. Thus we obtain a relatively smooth flux distribution (see the “Materials and Methods” section of Barabash et al., 2007 for technical details). MEX statistical studies have been made in the frame, refereed to IMF clock angle derived from MGS data. The reader can find details in Fedorov et al. (2006).

Fig. 2 shows a flow of heavy planetary ions behind the planet. Comparing solar wind flow distribution and planetary ions distribution we see that they are strictly complementary. In other words, high flux of planetary ions corresponds to low flux or absence of the solar wind. Note that in the case of Venus, the boundary of the planetary ion domain is more pronounced than at Mars because the ion gyroradius is more than four times smaller at Venus than at Mars for the same particle energy.

## 3. Shape of solar wind voids and its contents

We postulate that protons with energy greater than 300 eV are the signature of the planetary magnetosheath in the Mars or Venus downstream region (tailward from the planet). Fig. 1 then shows spatial distribution of solar wind flux tailward from Mars and Venus. Mars creates a solar wind void much larger than that of Venus when scaled by their respective planetary radii. This results from the larger scale of the Martian exosphere and lower solar wind pressure. However, this difference disappears if we plot these distributions in an absolute scale. The white dashed line in the left panel of Fig. 1 shows the approximate boundary of solar wind plasma in those particular

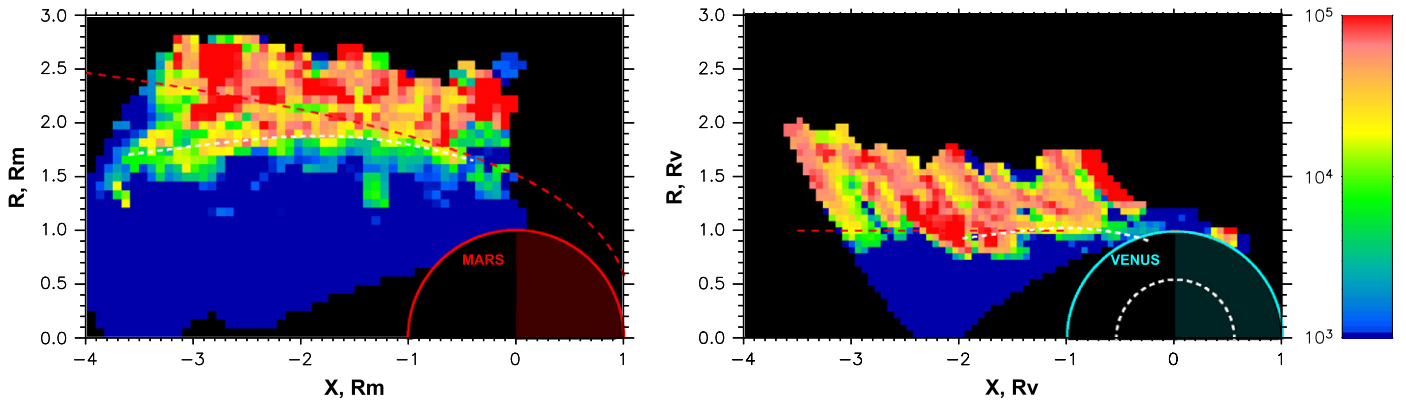


Fig. 1. Spatial distribution of the proton flux with energy greater than 300 eV in cylindrical coordinates:  $X$  connects the planet center and the Sun;  $R = \sqrt{Y^2 + Z^2}$ . All scales are in planet radii. The color scale is shown in arbitrary units. Blue color indicates zero flux, and black color shows the absence of the measurements. Left panel shows the Martian wake, and right panel shows the Venusian one. Red dashed curve in the left panel shows the theoretical position of the magnetosphere boundary after Kallio (1996). Similar dashed line in the right panel shows the wake boundary at Venus. White dashed curves are explained in the text.

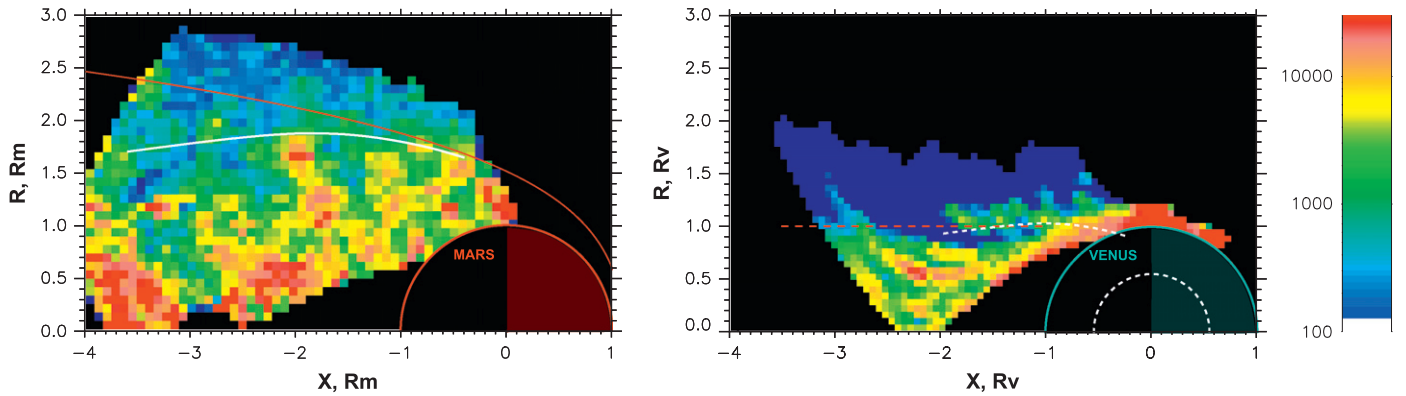


Fig. 2. The same as Fig. 1 but for ions of planetary origin with  $M/Q > 14$ .

statistics. The same curve is shown in the right panel but on the scale referred to the Venusian radius (Fig. 2).

#### 4. Energy distribution of planetary ions

As it was shown by Fedorov et al. (2006) and Dubinin et al. (2006), the planetary origin ions in the Martian wake exhibit an energy dispersion from the tail periphery down to the tail center. High energy ions are observed far from the center and low energy ions concentrate closer to the  $X$ -axis. Another important feature is an increase of the heavy ion energy inside the plasma sheet (PS) (see Dubinin et al., 1993; Kallio et al., 1995). PS is a thin layer of dense accelerated planetary plasma which spatially coincides with the current sheet of the magnetotail. If we create a special frame of reference (MSE) where  $Z_{\text{MSE}}$ -axis is parallel to the convective electric field of the solar wind ( $-V_{\text{cw}} \times B_{\text{IMF}}$ ) and  $X_{\text{MSE}}$  is the Sun-planet line, the current sheet would lie in the  $X_{\text{MSE}}, Z_{\text{MSE}}$  plane (see for instance Luhmann and Brace, 1991). The PS of the Martian magnetotail and both mentioned features of the ions energy are well seen in Fig. 3. PS manifests itself as a vertical bar of enhanced

heavy ions flux of about 1.2  $R_{\text{M}}$  width (left panel of Fig. 3). If we plot the heavy ions energy as a function of  $Y_{\text{MSE}}$  (Fig. 3, right panel) we will see a well-shaped profile. The  $|Y_{\text{MSE}}| > 0.6 R_{\text{M}}$  intervals show the energy slope starting at  $\sim 10000$  eV and falling down to the minimal measured energy (30 eV). The spatial interval  $|Y_{\text{MSE}}| < 0.6 R_{\text{M}}$  demonstrates a completely different plasma regime: a strong flux of ions between 200 and 2000 eV. This plasma regime corresponds to PS of magnetotail. Unfortunately we cannot provide a statistical analysis of the VEX data in VSE (like MSE) frame of reference yet. This will be a topic of a future investigation. Right now we just study the Venusian magnetotail ion energy as a function of  $R$ , where  $R = \sqrt{Y_{\text{VSO}}^2 + Z_{\text{VSO}}^2}$ . Fig. 4 shows the scatter plot of the energy of protons (both solar wind and planetary) and heavy ions.

One can see the shocked solar wind plasma at  $R > 1R_{\text{V}}$  (left panel). Another population distributes between 0 and  $1R_{\text{V}}$  and shows a small energy dispersion with the minimum at  $R = 0.5R_{\text{V}}$ . The dense cloud of the heavy ions events shows the same behavior (right panel, low-energy cutoff), but there are also heavy ion flows scattered

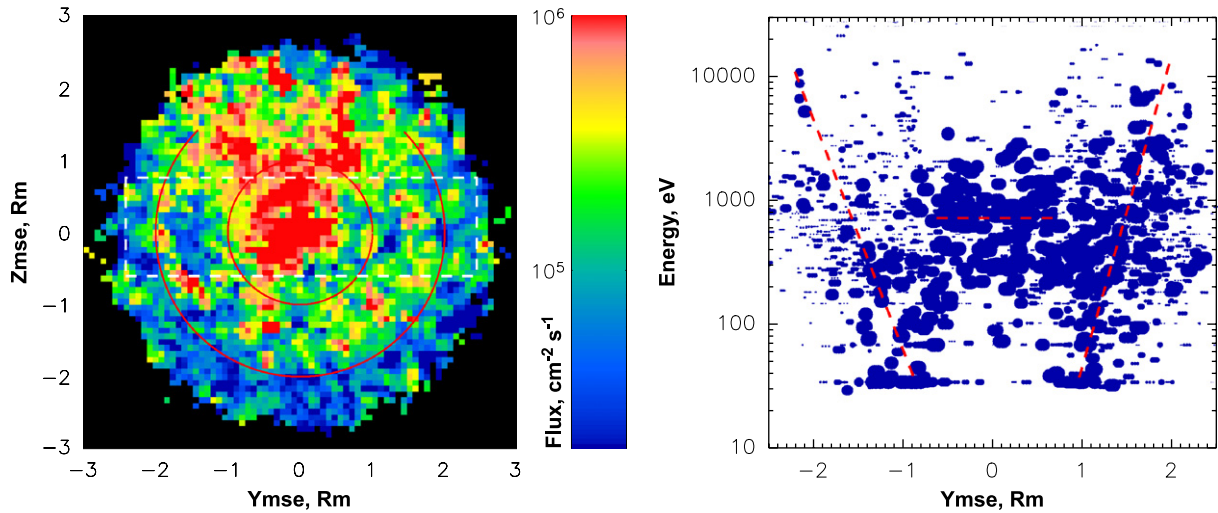


Fig. 3. Ion properties of the Martian magnetotail obtained from MEX Aspera-3 data. Left panel: distribution of the tailward flux of planetary ions of  $M/Q > 14$  in  $Y_{MSE}, Z_{MSE}$  plane. This plane is perpendicular to the Sun-planet axis.  $Z_{MSE}$  corresponds to the direction of convection electric field  $-V_{sw} \times B_{IMF}$ . Here  $V_{sw}$  is the solar wind velocity vector and  $B_{IMF}$  is the interplanetary magnetic field vector. See details in Fedorov et al. (2006) and Barabash et al. (2007). Right panel: scatter plot of planetary heavy ions energy as a function of  $Y_{MSE}$ . Samples have been picked inside the rectangular region shown in the left panel by white dashed line. Diameter of the circles corresponds to the ion flux on a logarithmic scale.

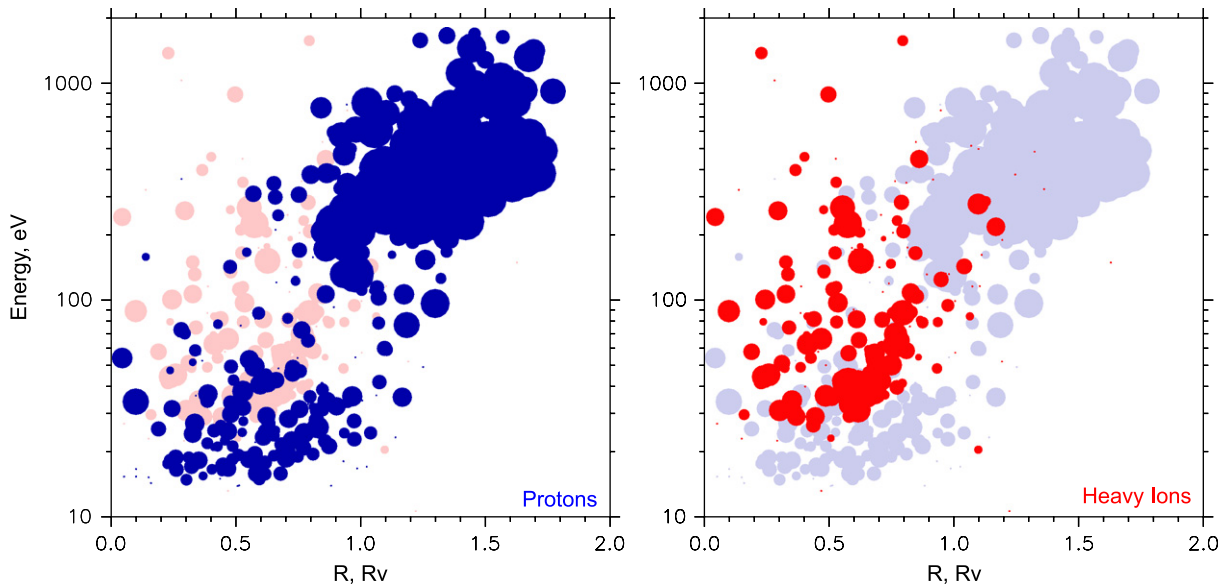


Fig. 4. Scatter plots of energies of  $H^+$  (left panel) and ions of  $M/Q > 14$  (right panel) as a function of the distance to the Sun-Venus line. Diameter of the circles corresponds to the ion flux in logarithmic scale (units are arbitrary). To simplify the comparison, the complementary distribution is shown in the each panel as a light background.

between 100 and 1000 eV. Comparing the left panels of Figs. 4 and 3, we can suppose that low energy dispersive part of heavy ions distribution in the Venusian tail corresponds to that observed in the Martian tail when  $|Y| > 0.6R_M$ . The scattered high energy part ( $> 100$  eV) corresponds to PS. This hypothesis should be proved by a future study. Note that only heavy ions demonstrate high energy flows in the center of Venusian tail.

Fig. 5 shows that on August 7, 2006 at 0156 UT VEX crossed the current sheet in the planetary tail (the distance

from the planet was about  $1R_V$  tailward). The signature of a current sheet is the abrupt change of  $B_x$  sign. The left panel of Fig. 5 shows that such  $B_x$  profile corresponds to the pass from one tail “lobe” to another. We see that  $B_x$  turn is associated with a bursty intense tailward flow of  $O^+$  of about 700 eV energy. It is consistent with the MEX observations. There are yet several important features that one can see in Fig. 5. (1) Current (and plasma) sheet coincides with minimum of energy and minimum of flux of  $H^+$  ions. (2) The current sheet is enveloped by thin layers of

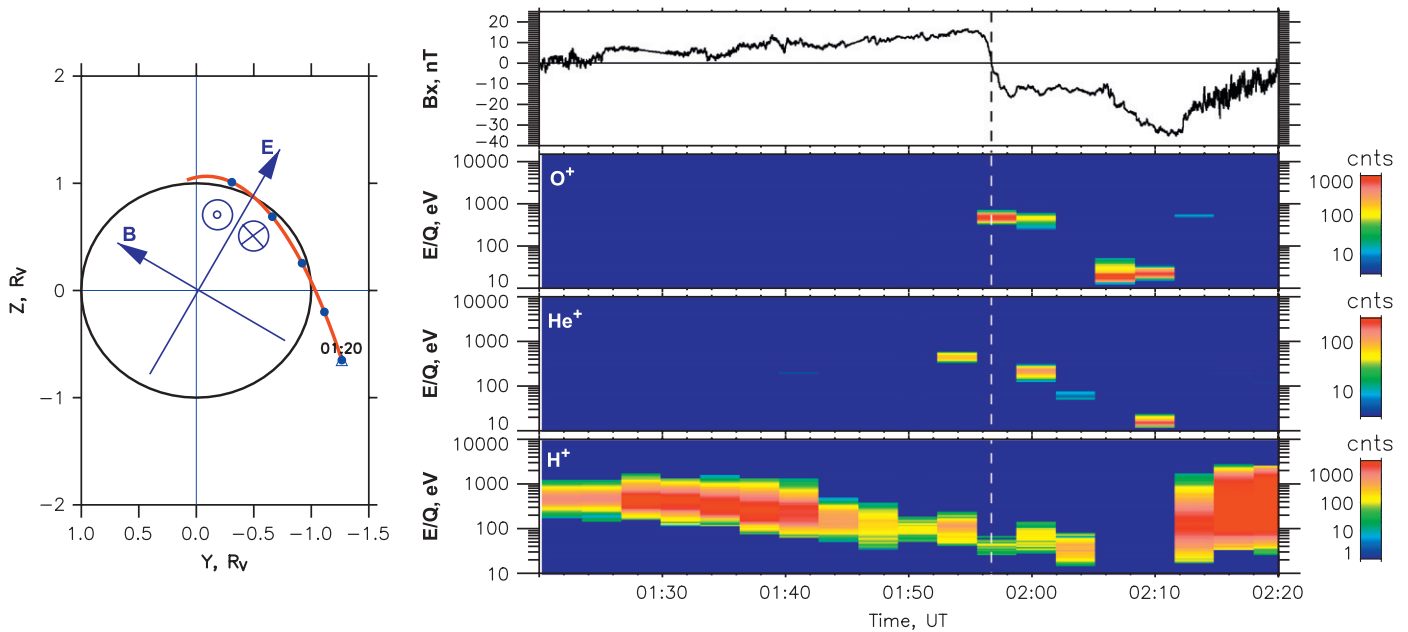


Fig. 5. Left panel: VEX orbit on August 7, 2006 in  $Y_{VSO}$ ,  $Z_{VSO}$  plane looking from the tail. Vector  $B$  shows the direction of the interplanetary magnetic field derived from magnetometer data. Vector  $E$  corresponds to the convective electric field  $-V_{sw} \times B$ . The circles with a cross and a point inside display the general direction of  $B_x$  on the both sides of the current sheet (see text for details). Right panel from top to bottom:  $B_x$  component of magnetic field. Energy-time spectrograms of  $O^+$ ,  $He^+$ , and  $H^+$  correspondingly. The vertical dashed line shows a current sheet crossing.

$He^+$  of medium (200–500 eV) energy. Both these very interesting features have not been observed near Mars, first of all because the IMA aboard of MEX cannot detect  $H^+$  less than 300 eV energy. The distribution of  $He^+$  in the Mars environment needs extra investigation.

## 5. Conclusions and future studies

Comparison of properties of downstream regions of Mars and Venus shows:

- (1) Solar wind voids are created behind both planets. The cross-section size of the voids is identical in the absolute scale. The Venusian void is close to the optical shadow of the planet. The transition from the magnetosheath plasma regime to the tail plasma regime is much sharper at Venus than at Mars.
- (2) Both voids are filled by accelerated planetary origin ions including  $H^+$ ,  $He^+$ ,  $O^+$ , and  $O_2^+$ .
- (3) Energy of  $H^+$  of planetary origin is high (several keV) at the periphery of the tail and goes to zero at plasma sheet in the tail center. This feature is observed at both planets.
- (4) Energy of heavy planetary ions demonstrates the same profile, but in the region of the cross-tail current sheet a thin layer of accelerated (500–1000 eV) heavy ions is observed (plasma sheet). This feature is identical for both planets.
- (5)  $H^+$  and  $He^+$  ions create an envelope around plasma sheet. A moderately accelerated layer of  $He^+$  is located between low energy  $H^+$  and accelerated  $O^+$  layers. This

feature has been observed in the Venusian tail only. This item should be proved by future statistical study.

In the near future we will complete the statistical investigation of plasma regimes in the Venusian tail in the IMF frame of reference. Then we will study  $He^+$  properties in the Martian and Venusian tails. The layered structure of the Venusian tail is the topic of special study.

## References

- Alfvén, H., 1957. On the theory of comet tails. *Tellus* 18, 92–96.
- Barabash, S., Lundin, R., Andersson, H., et al., 2004. The Analyzer of Space Plasmas and Energetic Atoms (ASPERA-3) for the European Mars Express Mission. ESA Publ. SP-1240, 121–139.
- Barabash, S., Fedorov, A., Lundin, R., Sauvaud, J.-A., 2007. Martian atmospheric erosion rates. *Science* 315, 501–503.
- Dubinin, E., Lundin, R., Norberg, O., Pissarenko, N., 1993. Ion acceleration in the Martian tail: Phobos observations. *J. Geophys. Res.* 98, 3991–3997.
- Dubinin, E., Lundin, R., Fränz, M., et al., 2006. Electric fields within the Martian magnetosphere and ion extraction: ASPERA-3 observations. *Icarus* 182 (2), 337–342.
- Fedorov, A., Budnik, E., Sauvaud, J.-A., et al., 2006. Structure of the martian wake. *Icarus* 182 (2), 329–336.
- Kallio, E., 1996. An empirical model of the solar wind flow around Mars. *J. Geophys. Res.* 101, 11133–11147.
- Kallio, E., Koskinen, H., Barabash, S., Nairn, C., Schwingschuh, K., 1995. Oxygen outflow in the Martian magnetotail. *Geophys. Res. Lett.* 22, 2449–2452.
- Luhmann, J.G., Brace, L.H., 1991. *Rev. Geophys.* 29, 121–140.
- Luhmann, J.G., Ledvina, S.A., Russell, C.T., 2004. Induced magnetospheres. *Adv. Space Res.* 33, 1905.
- Lundin, R., Zakharov, A., Pellinen, R., et al., 1998. First measurements of the ionospheric plasma escape from Mars. *Nature* 341, 609.

- McComas, D.J., Spence, H.E., Russell, C.T., Saunders, M.A., 1986. The average magnetic field draping and consistent plasma properties of the Venus magnetotail. *J. Geophys. Res.* 91, 7939–7953.
- Moore, K.R., McComas, D.J., Russell, C.T., Mihalov, J.D., 1990. A statistical study of ions and magnetic fields in the Venus magnetotail. *J. Geophys. Res.* 95, 12005–12018.
- Vaisberg, O.L., Zeleny, L.M., 1984. Formation of the plasma mantle in the Venusian magnetosphere. *Icarus* 58, 412.
- Vaisberg, O.L., Smirnov, V.N., Zastenker, G.N., Fedorov, A.O., 1989. Experimental data on the plasma shells of Mars, Venus, and Comets Halley and Giacobini–Zinner—comparison of loading effects. *Cosmic Res.* 27, 748.
- Zhang, T.L., Baumjohann, W., Delva, M., et al., 2006. Magnetic field investigation of the Venus plasma environment: expected new results from Venus Express. *Planet. Space Sci.* 54, 1336–1343.